Relating Power Draw and Fractal Dimension to Operation Parameters in a Lab-Scale Ball Mill

Iman Moradi, Ali Akbar Abdollahzadeh[1], Mehdi Irannajad

Department of Mining Engineering, Amirkabir University of Technology (Tehran Polytechnique), Tehran, Iran

Abstract

The goal of this study is to determine how the setting of operational parameters in a laboratory-scale ball mill affects the fractal dimension and power draw. The trials were designed using Design Expert software. Three optimization tests were used to evaluate the resultant mathematical model, and the results indicated that it had adequate validity. Percent solids, grinding time, and mill speed are operational parameters of the mill examined in this research. The results show that increasing the percent solids reduces both the fractal dimension and the amount of particles smaller than 25 microns. Increasing the solid content from 25 to 45 percent and from 45 to 65 percent results in increases and decreases in power draw, respectively. As the grinding time increased, the power draw reduced. On the other hand, the reduction ratio and weight of particles smaller than 25 microns and, consequently, the fractal dimension increased as grinding time increased. The findings suggest that a higher mill speed will lead to a greater power draw. The fractal dimension, reduction ratio, and weight of particles smaller than 25 microns will all rise if the mill speed is increased from 55% to 75% of the critical speed. Increasing mill speed from 75% to 95% only increases power draw without significantly affecting other parameters.

Keywords: Fractal dimension, Power draw, Grinding, Reduction ratio, Ball mill.

1. Introduction

Research indicates that energy efficiency in particle grinding within ball mills is low. A better understanding of ball mill operating parameters is necessary to boost their efficiency [1-5]. The operating parameters of ball mills are always determined experimentally, requiring a significant amount of time and effort [6]. Laboratory tests assessed the impact of grinding speed, particle and ball filling, ball size distribution, grinding aid dosage, and grinding duration on the particle size (d50, d80) and surface area (m^2/kg) of ground calcite ore [7]. Various studies have shown that the rotation speed of the mill plays an important role in grinding particles and energy consumption [8]. The rotation speed depends on the purpose of grinding particles, ore, and the size of the ball load. Increasing the rotation speed increases energy efficiency because the impact mechanism plays a more important role in particle breakage. On the other hand, by increasing the rotation speed too much, the efficiency of the mill decreases due to the centrifugation of the balls. Reducing the rotation speed also increases energy efficiency but reduces the capacity of the mill [9]. For particle grinding, several studies have found that the best results are obtained at varying speeds, ranging from 65% to 85% of the critical speed [10], 85% of the critical speed [11], and less than 90% of the critical speed [12]. A factor that influences wet grinding efficiency is the percentage of solids. On iron ore, solids percentages ranging from 72% to 82% were examined; the findings indicate that a higher solids percentage elevated the slope of the breaking rate curve [13]. When pebbles were used as the grinding media, solid percentages ranging from 65% to 75% were examined. The findings indicated that greater solids percentages led to increased rates of breakage for coarse particles [14]. In one study, the solids percentage was reduced from 83% to between 76% and 80%, and by keeping the output granulation conditions constant, the mill capacity increased by 10%, and the energy consumption was also reduced [15]. According to research, the grinding efficiency was maximum at 70% solids. As the solids percentage increased to 80%, it decreased significantly during long-term grinding due to the increase in pulp viscosity

[1]Corresponding author: Ali A. Abdollahzadeh; E-mail: abdzad@aut.ac.ir; Tel: +98-2164545581, Tehran, Iran

[16, 17]. Additionally, it was discovered that variations in the pulp's solids percentage significantly impact the movement of the ball load within the mill. The center of gravity and dynamic regime of the ball load can be altered by variations in pulp viscosity brought on by variations in the solids percentage [18]. Research on industrial grinding has shown that the residence time of the materials in the mill is not very effective at high feed flow rates, but it has a significant impact on the performance of the mill at low feed rates [19]. Research has also shown that residence time affects the flow regime and rheology of the slurry [20, 21]. In an industrial case study, the findings showed that both the ball loading and the solid percentage of the slurry affected the retention time [22].

Energy consumption, power consumption, breakage ratio, product sizes, and product particle size dispersion are the most crucial factors to consider when assessing the performance of ball mills. The amount of energy and power that is used and dissipated has been calculated in recent years using a variety of techniques. Methods include Fractal [23], Discrete Element Methods (DEM) [24], Kick, Bond, and Rettinger [25, 26], and others (Rose and Evans [27], Morrell [28], Moys [29], Van Nierop et al. [30]). To describe the particle size distribution of crushed particles, statistical methods [31-33] such as normal distribution, Gates-Gaudin-Schuhmann, and Rosin-Rammler, or modern methods such as fractal geometry [34-39], machine vision, image analysis, and neural networks are used [40].

Nature's intricacies and imperfections are described by fractal geometry. It has been investigated to characterize the shape, size distribution, and surface morphology of particles. Fractal dimension, a scale-independent constant, has definite benefits for characterizing data at various sizes [41-43]. In a study, fractal geometry was used to describe the particle size distribution of several different chromite ores. Various equipment was used to crush the ores. The results obtained for fractal dimension show that the type of equipment and ore have a significant effect on the particle size distribution [44]. Using the fractal dimension, the impact of feed, particle size, and ore type on the distribution of particle sizes in dry ball mill products was examined. The findings demonstrated that the fractal dimension is directly correlated with coarsening feed size and inversely correlated with rising feed weight. The fractal dimension is also significantly influenced by the type of ore, according to the data [45]. Fractal geometry was used to examine how the size distribution and form of the particles from wet and dry milling affected the wet magnetic separator. The findings demonstrated that higher-grade magnetic separator products and particles with bigger fractal dimensions were created by dry milling [46, 47]. Fractal geometry was used to examine how wet grinding affected the morphology of the particles and how it affected flotation performance. There is a direct correlation between flotation recovery and fractal dimension, according to the data collected [48].

It should be highlighted that fractal behavior is not always present in the phenomena being studied. Some fractal geometry techniques require that the fractal dimensions be within a specific range; if they are outside of this range, the phenomena being studied do not exhibit fractal behavior. When examining the particle size distribution, the fractal dimensions must fall between two and three. The fractal dimensions of certain recent studies on the particle size distribution after crushing and grinding were beyond the intended range. Therefore, it was concluded that there was no fractal activity in the samples and settings under investigation [49, 50].

Ore grinding is a complex and irregular process. However, fractal geometry has also been created to investigate irregular and complicated processes. Thus, the grinding process may be described using fractal geometry. It is evident from the examined literature that there hasn't been much study done on how ball mill operating settings affect particle size distribution with fractal geometry. Thus, the goal of this study is to examine how operational factors affect the fractal dimension derived from variations in the particle size distribution. Additionally, the impact of these characteristics on variations in power draw has been examined. In a previous study, the authors looked at how ball size (BS), fractional ball filling (FBF), and particle filling (PF) influenced the particle size distribution (PSD) using the fractal dimension (Df) and power consumption [51]. The results demonstrate that when the fractal dimension is at its maximum, the ball mill runs more power-efficiently. Because of this, the authors modified the performance settings of the wet ball mill for these parameters. The optimal values for the parameters FBF, PF, and BS were 17.62%, 60%, and 19.05 mm, respectively [51]. Therefore, the investigation employs these optimal values. Grinding time, speed, and solid percentage have all been examined in this study as a continuation of earlier research and to finish optimizing the factors influencing the ball mill's performance. Iron ore from the Gol Gohar mine in Sirjan was the sample of this study. Samples of dry magnetic separator tailings and input to regrinding mills were produced since the goal was to examine the performance of regrinding mills.

2. Materials and Methodology

2.1. Material

The sample's chemical composition, mineralogy, and particle size distribution were examined to learn more about the materials used in this investigation. According to the particle size distribution, the feed's D_{80} was 380 microns. The sample's mineralogy was analyzed using X-ray diffraction (XRD). The results indicated that magnetite, lizardite, and pyrite were the primary minerals found in the sample. The sample's chemical composition was determined using X-ray fluorescence (XRF), and the results showed that the primary constituents of the sample were Fe_2O_3, Si_2O, MgO, Al_2O_3, and S.

2.2. Milling

In this investigation, a ball mill jar was used. The instrument is equipped with an online data logging system. The power drawing system records the mill's power demand every ten seconds. Table 1 shows the specifications for the feed and the ball mill. Milled particle size distribution was analyzed using sieves with mesh sizes of 300, 150, 106, 90, 83, 75, 63, 53, 45, 37, and 25 microns. The ball size, particle filling, and ball filling were 19.05 mm, 60%, and 17.62%, respectively.

Table 1- Specifications of the ball mill and feed

Mill	Inner diameter, D (mm)	200
	Length, L (mm)	200
	Volume, V (cm3)	6283
	Critical speed, Nc (rpm)	94
	Operational speed (55, 65, 75, 85, and 95% of critical speed) (rpm)	52, 61, 71, 80, and 89
	Fractional ball filling, J	0.1762[a]
	Void between balls (cm^3)	442.8[b]
Ball	Material	Manganese Steel
	diameter (mm)	19.05
	Specific gravity (gr/cm3)	7.5
Feed Material	Specific gravity (gr/cm3)	4.12
	Feed size (mm)	0 -1

[a] $Fractional\ ball\ filling, J = \left[\left({}^{mass\ of\ balls}/_{ball\ density} \right) /_{mill\ volume} \right] * [{}^{1}/_{0.6}]$ [44]

[b] $Void\ bettween\ balls = [J * (mill\ volume)] - [volume\ of\ balls]$ [44]

2.3.Fractal Dimension

Fractal geometry can be used as a method for linearizing and describing particle size distributions. To investigate the particle size distribution using fractal geometry, a relationship between particle size and weight is constructed using formula (3) [52-55]:

$$\frac{M(X < x)}{M_T} = (\frac{x}{X_L})^{(3-D_f)} \quad (1)$$

Where XL is the size of the largest dimensional fraction, Df is the fractal dimension, MT is the weight of the entire sample, and x is the size of each dimensional fraction. The total weight of particles moving through each dimensional fraction is denoted by the letter M(X< x). Relation (1)'s logarithmic translation for a scale-invariant (fractal) PSD results in a linear relationship between M(X< x)/MT and x/XL:

$$ln\frac{M(X < x)}{M_T} = \left(3 - D_f\right)\ln(\frac{x}{X_L}) \quad (2)$$

The slope coefficient (m) for the linear regression line was derived using the linear best fit of the relationship (2), and Df is computed using the equation.

$$D_f = 3 - m \quad (3)$$

This approach restricts the fractal dimension of the fragmentation to (0 < Df < 3). This approach yields a comminution metric that may be used to determine the fractal dimension. The experimental conditions of comminution are typically moderate (Df≈2.5). With relatively few values lying outside of this range, comminution investigations often provide results in the 2 < Df < 3 region. The energy dissipation will therefore take place in a fractal domain between a surface (Df=2) and a volume (Df=3). A fractal dimension (Df) of 2 and 3 loses energy since the pieces are self-similar at all sizes [56-58].

Relation (1) is similar in form to the wide PSD proposed by the Gates–Gaudin–Schuhman (GGS) distribution function: M = 100*(x/k)a, where “x” is the screen size, “M” is the cumulative percentage finer than x, “a” is the uniformity index, and “k” is the size parameter. This suggests that the GGS line's slope “a” equals 3 _ Df and that the GGS equation is fractal [57, 58]. Theoretically, smaller values of "a" would suggest more coarse particles, more fines, and fewer medium-range particles [59, 60].

3. Experimental design

In this work, the central composite technique, a well-liked response surface methodology, was used to apply three parameters to the fineware on three distinct surfaces (see Table 2). Fractal dimension and power draw were the response variables, while solid percentage, speed, and time were taken into account when constructing the tests. The central composite technique was used to construct twenty tests with six central points each.

Table 2- Initial conditions for performing the test

Index	Name	Units	Low	High	-alpha	+alpha
A	Solid percentage (S.W.P)	%	35	55	25	65
B	Time (t)	Min	10	25	5	25
C	Speed (S)	Rpm	65	85	55	95

The fineware received the power draw and fractal dimension data as inputs. The analysis of variance (ANOVA) approach was then used to find a suitable model for the answer. It has been confirmed that the model used in line with Tables 3 and 4 is correct. Equations 4 and 5, which are expressed in terms of coded factors, illustrate the fractal dimension and power draw model as well as the relationships between various parameters. These equations reflect the speed parameter, C, the time, B, and the solid percentage parameter, A.

Table 3- The model's accuracy coefficient for each of the examined samples

Response	accuracy coefficient		
Power draw	Adeq precision	Mean	Std. Dev
	19.80	1493.70	34.89
	Adj R-Squared	C.V	R-Squared
	0.9276	2.34	0.9695
Fractal Dimension	Adeq precision	Mean	Std. Dev
	19.92	2.69	0.036
	Adj R-Squared	C.V	R-Squared
	0.9013	1.35	0.9722

Table 4- ANOVA for the investigated sample's responses model

Response	ANOVA parameters			
Power draw	Source	Sum of squares	Df	Lack of Fit
	Model	0.0000309	11	0.7731 (not significant)
	Mean square	P-value Prob> F	F-value	
	28142.59	<0.0001 (significant)	23.12	
Fractal Dimension	Source	Sum of squares	Df	Lack of Fit
	Model	0.37	11	0.9083 (not significant)
	Mean square	P-value Prob> F	F-value	
	0.034	<0.0001 (significant)	25.45	

$$P.D = +1521.50 + 8.12A - 24.75B + 133.75C - 7.75AB + 1.50AC - 3.50BC - 23.75ABC \quad (4)$$

$$D_f = +2.73 - 0.054A + 0.14B + 0.028C + 0.034AB + 0.011AC - 0.014BC \quad (5)$$

4. Results and Discussion

To determine the ideal power draw for the lab-scale ball mill, the solid percentage, speed, grinding time, and mill operational parameters were examined. Several aspects of the milling process optimization were examined, including power draw, fractal dimension, reduction ratio (F80/P80), and the weight of particles smaller than 25 microns.

4.1. Effect of solid percentage

Optimizing mill power draw is a constant challenge in mineral processing. The power draw of mills is influenced by several factors. Time, speed, and solid percentage are the three characteristics that are examined in this study. The power draw changes caused by variations in the solid percentage are displayed in Figure 1a. The results show that excessive reduction or increase in the solid percentage does not affect the power draw of the mill. However, the reduction ratio when the solid percentage is 25% greater than 65%, decreases from 6.59 to 5.67 (see Table 5). When the solid percentage was 45% (6 center points), the power draw of the mill increased, in the range of 1471 to 1574 watts. On the other hand, the reduction ratio also increased, in the range of 7.25 to 7.82. On the other hand, the particle size distribution was investigated using the fractal dimension. The variation of the fractal dimension vs the solid percentage is shown in Figure 1b. The results show that increasing the solid percentage from 25 to 65 percent reduces the fractal dimension from 2.79 to 2.59. In other words, there is an inverse relationship between fractal dimension and solid percentage. Table 5 presents the overall results of the fractal dimension.

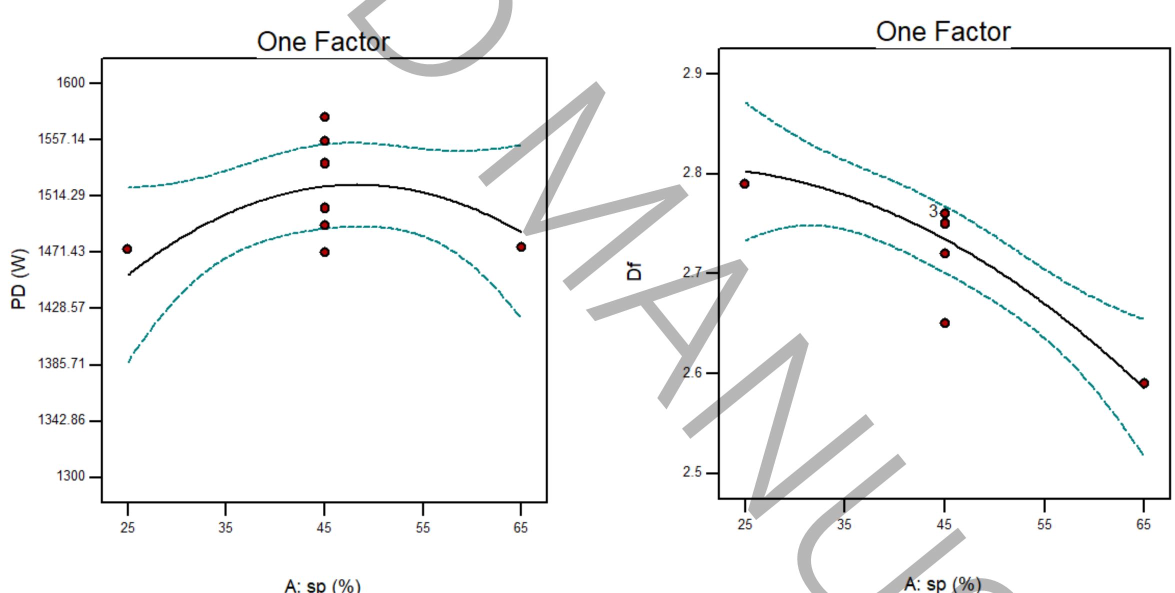

(a) (b)

Figure 1—Power draw and fractal dimension variations vs solid percentage changes

Table 5—Overall power draw and fractal dimension results based on mill operating parameters

Run	Solid percentage (%)	% of critical Speed (rpm)	Grinding time (min)	Power draw (W)	Fractal dimension	Weight percentage passing 25 microns (%)	Reduction ratio ($\frac{F_{80}}{P_{80}}$)
1	55	65 (61 rpm)	10	1371	2.42	25.61	3.87
2	45	75 (71 rpm)	15	1505	2.76	52.78	7.61
3	35	85 (80 rpm)	10	1586	2.70	45.35	6.29
4	35	65 (61 rpm)	10	1374	2.63	38.07	5.29
5	35	65 (61 rpm)	20	1307	2.81	60.26	7.44

6	55	85 (80 rpm)	20	1572	2.80	57.01	8.48
7	55	65 (61 rpm)	20	1368	2.74	48.84	7.51
8	45	95 (89 rpm)	15	1741	2.76	51.17	7.97
9	45	75 (71 rpm)	15	1471	2.76	52.27	7.69
10	45	75 (71 rpm)	15	1492	2.75	50.45	7.42
11	45	75 (71 rpm)	15	1539	2.76	52.57	7.82
12	45	75 (71 rpm)	15	1556	2.65	37.33	7.35
13	45	75 (71 rpm)	15	1574	2.72	47.78	7.25
14	55	85 (80 rpm)	10	1684	2.54	32.11	5.38
15	35	85 (80 rpm)	20	1600	2.83	63.38	8.02
16	65	75 (71 rpm)	15	1475	2.59	36.35	5.67
17	25	75 (71 rpm)	15	1474	2.79	57.23	6.59
18	45	75 (71 rpm)	25	1452	2.85	65.43	9.04
19	45	55 (52 rpm)	15	1182	2.67	40.83	6.35
20	45	75 (71 rpm)	5	1551	2.29	19.45	3.33

A decrease in the solid percentage means that the dilution has increased. When the dilution increases, fine particles float on the surface of the water, and the accumulation of particles in the toe area decreases [61]. Given that the most common grinding mechanism in the toe area is impact [62]. Therefore, larger particles that require an impact mechanism for grinding will not be crushed under these conditions, and the particle size distribution resulting from the grinding operation will become coarser (see Figure 2). However, lowering the percentage of solids increases the likelihood of fine particle fragmentation, which produces more tiny particles (-25 microns) (Figure 2). This is because fine particles gather in the abrasion zone, which is ideal for grinding fine particles and may result in the production of even finer particles. The fractal dimension increases as the weight of particles in the fine fractions increases. It is evident from Table 5's data that the weight of -25 micron particles decreases from 57.23% to 36.35% when the solid percentage is raised from 25% to 65%.

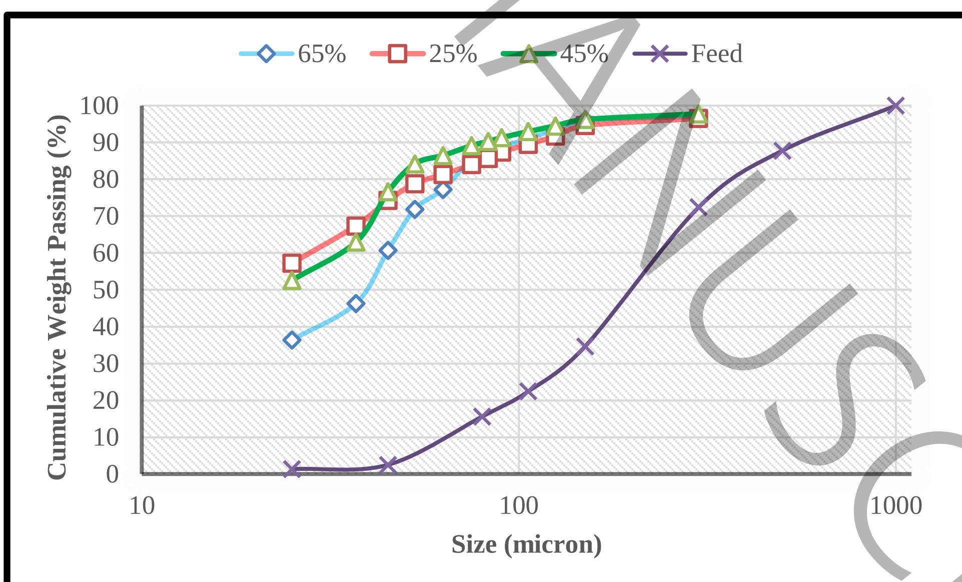

Figure 2—Particle size distribution resulting from grinding by solid percentages of 25, 45, and 65%.

The grinding power draw has decreased as a result of the solid percentage decline; this might be mostly attributed to a drop in the weight of the mill's contents. As the solid percentage increases, the balls become trapped in the pulp. This prevents the balls from participating in the cataracting movement and disrupts the impact mechanism in the mill. As the impact mechanism is disrupted, the coarse particles are not crushed, and as a result, the particle size distribution of the mill output becomes coarser. Also, as the solid percentage increases, a portion of the pulp is placed in the shoulder area, which participates in the cataracting movement and reduces the effect of the energy from the impact mechanism on the coarse particles. Therefore, the particles resulting from the grinding will be coarser. As the solid percentage increases, a layer of material develops around the balls. Consequently, the ball-material-ball collision loses its effectiveness, which lowers particle grinding. Additionally, this keeps the balls from striking the mill wall directly. On the other hand, it lessens the force of the hits with the wall, which lowers the mill's power draw. The results obtained are consistent with previous studies [13, 14, 61]. However, one study has shown that there is a relationship between pulp filling and pulp solids concentration. When the slurry filling is high, a lower percentage of pulp solids concentration leads to the production of more fine particles, and when the slurry filling is low, a higher percentage of pulp solids concentration leads to the production of more fine particles [15].

4.2. Effect of grinding time

The grinding time was another parameter that was looked at. Figure 3a displays the mill power draw results as a function of time. The findings indicate that the mill power draw dropped from 1551 to 1452 watts as the time grew from 5 to 25 minutes. The rheology of the pulp varies with increasing grinding time, which may have an impact on the mill's power draw. In ball mills, the quantity of fine particles rises because the coarse and fine particles are always crushed at the same time. During mill operation, fine particles often have a higher propensity to stay in a clump [63]. Thus, more fine particles will accumulate in the cascade and cataract sections. The balls involved in these two motions (impact mechanism) will also not collide with the mill wall as much, which will cause the mill to vibrate less and reduce its power draw. The change in fractal dimension over time is seen in Figure 3b. The findings indicate that the fractal dimension rises from 2.29 to 2.85 when the grinding duration is extended from 5 to 25 minutes.

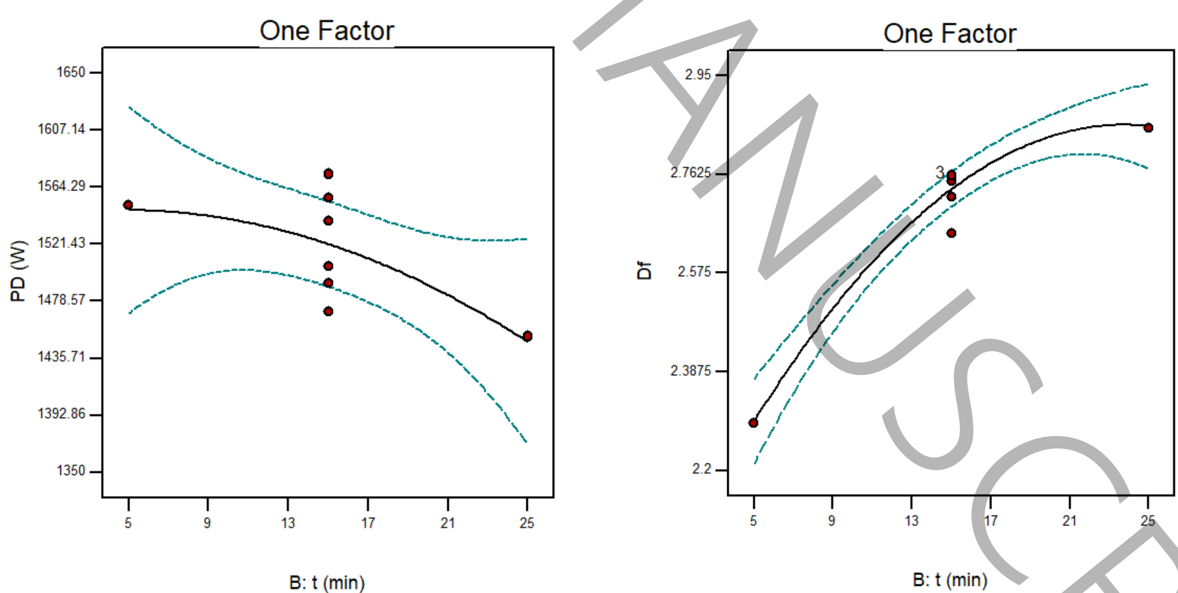

(a) (b)

Figure 3—Power draw and fractal dimension variations vs time changes

When the grinding time is 5 minutes, a large number of coarse particles are not crushed. In the cataract movement, these particles separate from the balls [63]. As a result, the balls will collide more with the wall of the mill, which will increase its vibration and power draw. Figure 4 illustrates the mill's power draw over a period of 5 minutes. This figure shows that the mill's power draw is high for 150 seconds and then drops sharply.

A 5-minute experiment was carried out to examine the power consumption needed for empty grinding, which occurs when there is no ball load, water, or particles present. Figure 4 displays the data, which indicate that empty grinding accounted for 68.80% of the power usage. It is important to remember that the percentage will vary based on the various ball-filling circumstances, rotation speed, and particle filling. Overall, the findings indicated that empty grinding accounts for 60–70% of power usage.

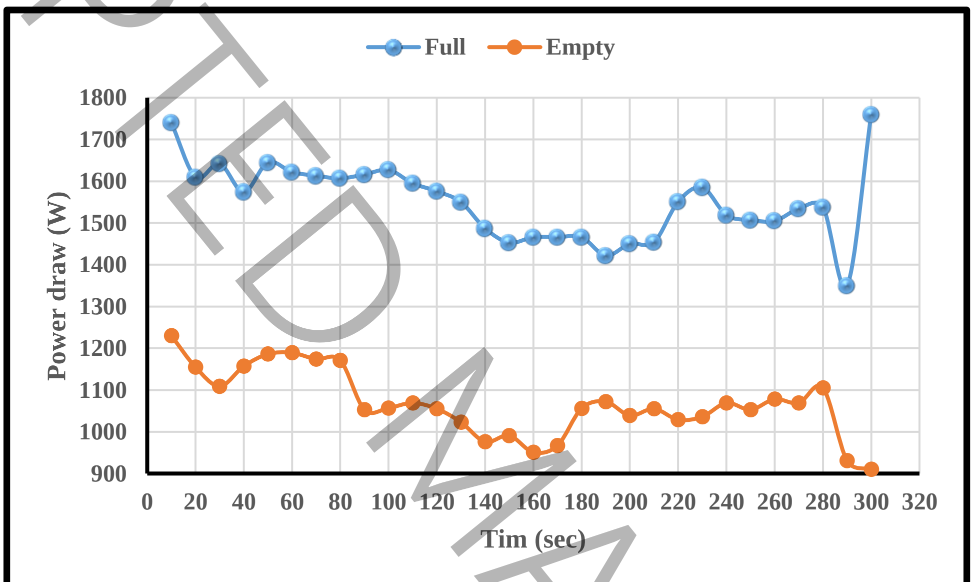

Figure 4—Changes in mill power draw over time for a grinding time of 5 minutes

Table 5 makes it evident that the reduction ratio rose from 3.33 to 9.04 when the grinding duration was extended from 5 to 25 minutes. Figure 5 shows the distribution of particle sizes as a consequence of the grinding times. When the grinding time increases from 5 to 25 minutes, the weight of -25 micron particles increases from 19.45 to 65.43 percent. Therefore, an increase in the grinding time leads to an increase in the reduction ratio despite a reduction in power draw. As previously shown, there is a direct relationship between grinding time and fractal dimension. The reason is that in a ball mill, fine particles are constantly being formed, and particles of different sizes are being crushed. Hence, increasing the grinding time will lead to an increase in fine particles and, consequently, fractal dimension.

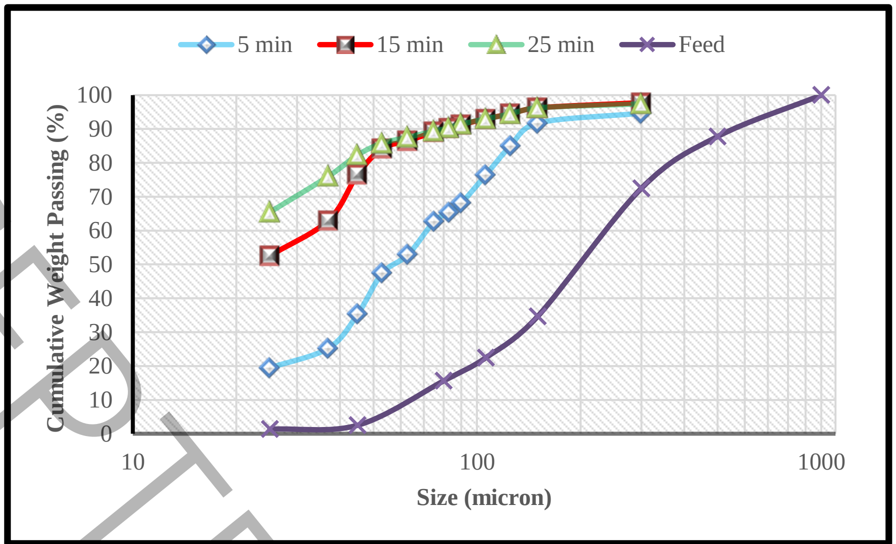

Figure 5—Particle size distribution after 5, 15, and 25 minutes of grinding

4.3. Effect of speed

Figure 6a shows how power draw is affected by mill rotation speed. The mill power draw rose from 1182 to 1742 watts when the mill speed was raised from 55% of the critical speed (52 rpm) to 95% of the critical speed (89 rpm), according to the data. Inconsistencies exist between the findings and some earlier research [10, 12, 64]. The results align with another study, however [9]. One probable explanation is that when the mill's speed rises, more balls may be travelling in a cataractous motion. When the speed increases, it produces more rotations within a specific time frame. The mill wall sustains more hits as a result of this increase, which raises the mill's vibration and, ultimately, its power draw. Figure 6b shows the results of the fractal dimension as a percentage of critical speed. The results show that the fractal dimension increased from 2.67 to 2.76 when the grinding speed increased from 55 to 95% of critical speed. This is because the weight of fine particles (-25 microns) increased from 40.83 to 51.17% as the mill speed increased from 55 to 95% of the critical speed.

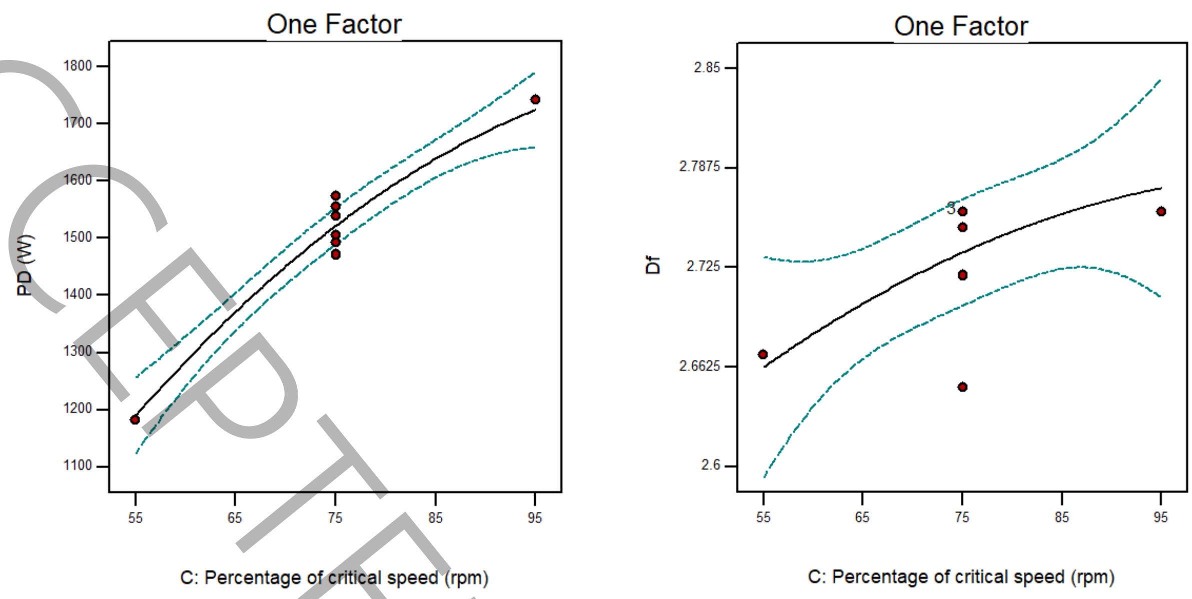

(a) (b)

Figure 6—Power draw and fractal dimension variations vs speed changes

Examining the findings in Table 5 and Figure 7, it is evident that the reduction ratio rose from 6.35 to 7.97 when the mill speed was raised from 55% (52 rpm) to 95% (89 rpm) of the critical speed. The reduction ratio was also between 7.25 and 7.82 when the mill speed was 45% of the critical speed. It follows that there was little change in the reduction ratio when the mill speed was raised from 75% to 95% of the critical speed. When the mill speed was increased from 75% to 95% of the critical speed, neither the fractal dimension nor the generation of fine particles (-25 microns) changed, nor did the increase in mill speed have a positive impact on these two parameters. This may be because some of the balls were ejected or centrifuged to a place further away in the cataract action that was higher above the pulp surface, making them useless for grinding material. The power draw of the mill has grown between 10.61% and 18.35%, as can be shown by comparing the power draw derived from speeds of 75% and 95% of the critical speed. The ideal mill rotation speed is thus 75% of the critical speed.

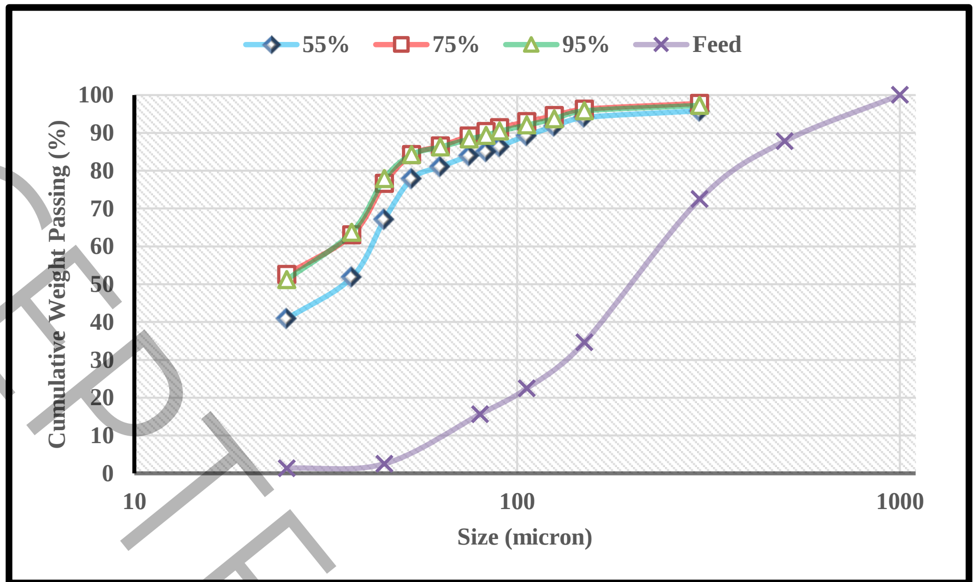

Figure 7—Particle size distribution from grinding at 55%, 75%, and 95% of the critical speed

4.4. Interaction of parameters

Optimizing the power draw, particle size distribution, and fractal dimension requires an understanding of how ball mill operating parameters interact. The relationship between operational parameters and power draw fluctuation is seen in Figure 8.

A look at Figure 8a demonstrates that lowering the solid percentage and lengthening the grinding time will result in a lower power draw. This is because lowering the solid percentage will result in a lower weight of the mill's contents. Conversely, more fine particles will be produced if the solid percentage is decreased and the grinding duration is extended. Rheological changes alter the pulp's viscosity, reducing the balls' involvement in the cascade motion. This also lessens the likelihood that the balls will collide with the mill wall during the impact mechanism, which lowers the mill's vibration and, ultimately, its power draw.

According to the findings, power draw is most impacted by mill speed (see Figures 8b and c). As the mill speed increases, the balls travel more quickly, which causes some of them to be flung farther. The mill vibrates more and consumes more power as a result of the increased impact of the balls on the mill wall. Increased mill speed, on the other hand, tilts the pulp toward the shoulder, reducing the pulp surface area at the toe and increasing the balls' impact on the wall.

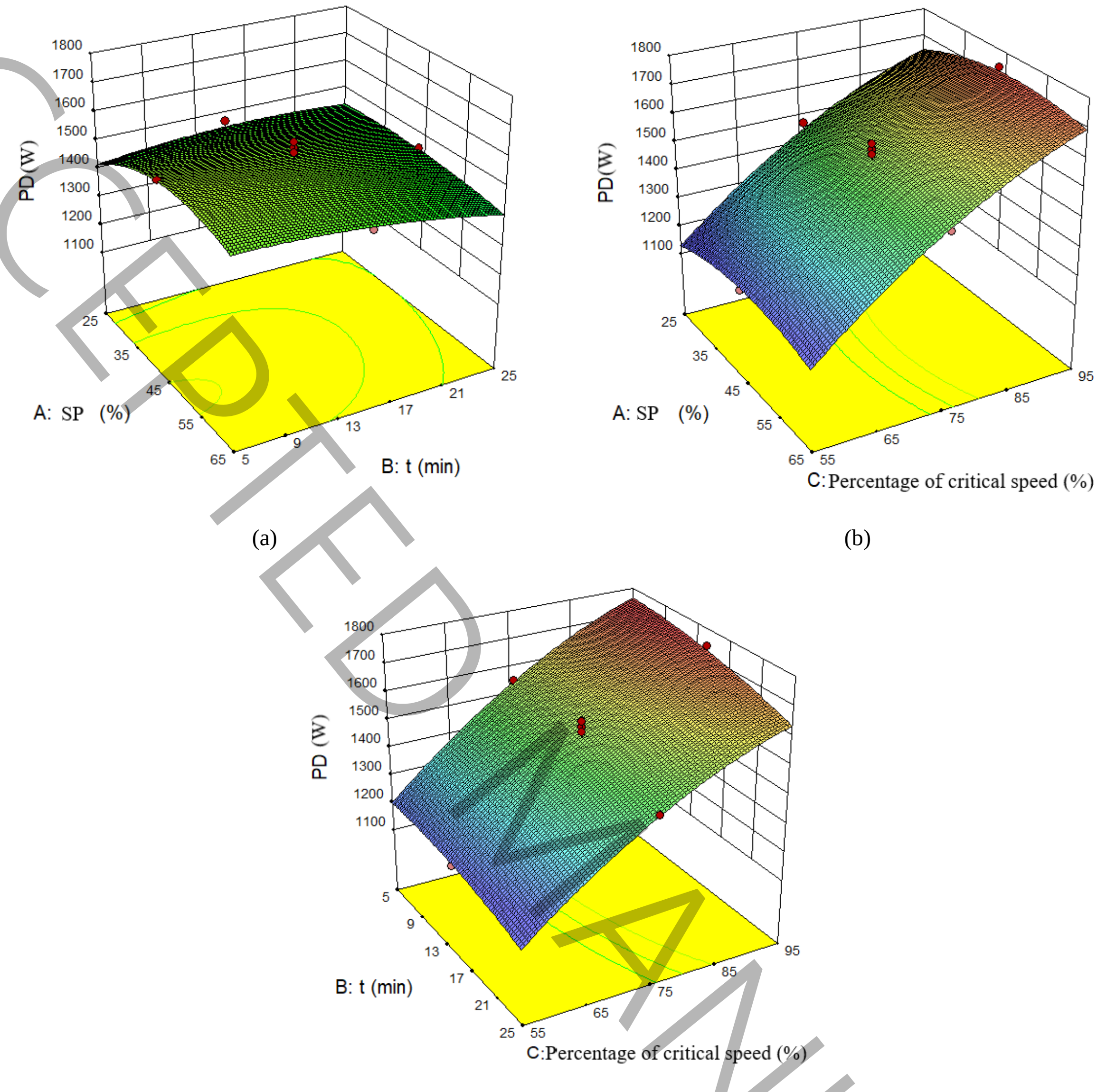

Figure 8—Effect of interaction of mill operating parameters on power draw

Figure 9 shows the interaction effect of mill operating parameters on fractal dimensions. Unlike the power draw, which is strongly influenced by mill speed, the fractal dimension is influenced by all parameters, and each parameter has a greater effect on it at a certain range. Examination of Figure 9a shows that decreasing the grinding time harms the fractal dimension, such that increasing or decreasing the solid percentage does not affect the fractal dimension. On the other hand, the highest fractal dimension is obtained when the solid percentage is about 55% and the grinding time is 25 minutes.

Figure 9b illustrates how the parameters of solid percentage and critical speed percentage interact to produce a fractal dimension. The highest fractal dimension is produced by the lowest solid percentage (25%) and the highest mill speed (95% of critical speed); on the other hand, the lowest fractal dimension is produced when the solid percentage reaches its maximum value (65%) and the mill speed reaches its minimum value (55% of critical speed).

Reducing or raising the mill speed has little impact on the fractal dimension when the grinding time is 5 minutes, as Figure 9c demonstrates. The largest fractal dimension will be obtained, nonetheless, if the time is extended to 25 minutes at all speeds.

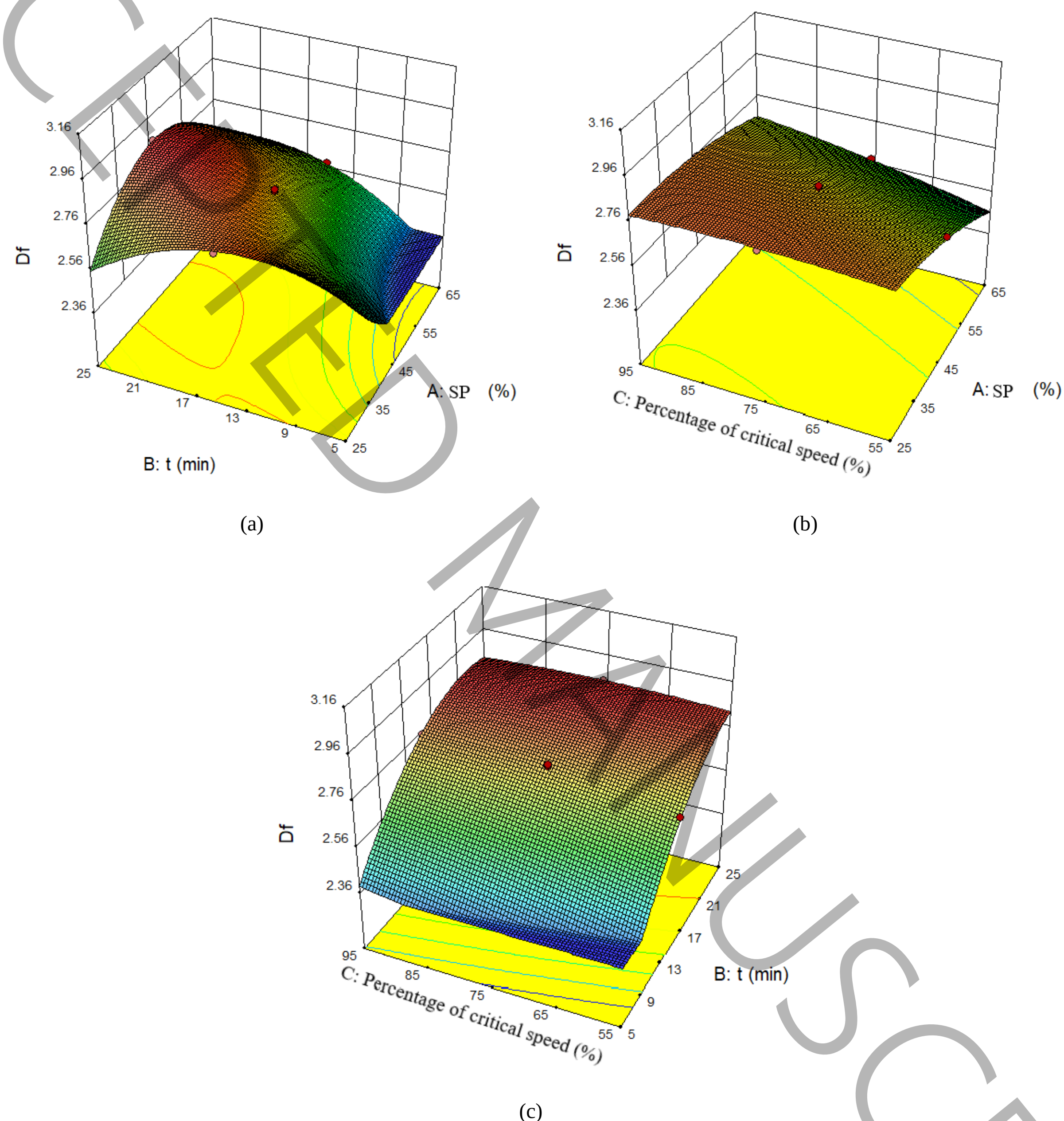

Figure 9—Effect of interaction of mill operating parameters on fractal dimension

4.5. Optimization

The software has conducted numerous tests under specific conditions to scrutinize and confirm the obtained models. The objective was to achieve a greater fractal dimension. Thus, in the software, the fractal dimension was chosen in its maximum state, and the operational parameters of solid percentage, grinding time, percentage of critical speed, and power draw were chosen within the range. Table 6 displays ideal circumstances as recommended by the software. According to the data shown in Table 6, the ideal circumstances for the solid percentage, grinding time, and percentage of critical speed were 43.62%, 20 minutes, and 85%, respectively. Conversely, the coefficients of desirability, fractal dimension, and power draw were 0.992, 2.85, and 1608 W, respectively.

The results obtained from the three optimization tests are presented in Table 7. The fractal dimension results obtained for tests 1, 2, and 3 were 2.81, 2.83, and 2.85, respectively. The results obtained were consistent with the predicted results, within a 95% confidence level. However, this table also presents the power draw results. The results obtained show that the power draw of the optimization tests is not consistent with the software prediction and is not within the 95% confidence level. However, since the power draw obtained is less than the predicted values, the results are desirable, and the energy consumption is more optimally used.

Table 6- Optimal conditions for grinding

Parameter	Solid percentage (%)	Grinding time (min)	Percentage of critical Speed (%)
Optimization	43.62	20	85
Power draw (W)	1608		
Fractal dimension	2.85		
Desirability	0.992		

Table 7- Results of actual and predicted optimal conditions

Response	Number	Actual values	Predicted values at 95% confidence level
Power draw (W)	1	1432	1558-1658
	2	1333	
	3	1360	
Fractal dimension	1	2.81	2.79-2.90
	2	2.83	
	3	2.85	

5. Conclusion

This study investigated the impact of solid percentage, grinding time, and mill speed on fractal dimensions and power draw. The findings are presented below:

- The fractal dimension findings are in line with the fractal geometry principle, which says that the ground's particle size distribution between 2 and 3 determines the fractal dimension. The fractal dimension values in this investigation ranged from 2.29 to 2.85.
- The mill power draw was about the same for both, and the adjustment in the solid percentage from 25 to 65% had no impact. When the solid percentage hit 45% under the identical circumstances, the power draw rose. Fractal dimension and solid percentage, however, were inversely correlated.
- As the solid percentage rose from 25 to 45%, the reduction ratio rose; however, as the solid percentage rose from 45 to 65%, the reduction ratio fell. Nonetheless, the proportion of particles smaller than 25 microns consistently dropped as the solid percentage rose.
- The power draw decreased with increasing grinding time. However, increasing grinding time resulted in an increase in fractal dimension, reduction ratio, and the weight content of particles smaller than 25 microns.
- The results show that increasing the mill speed will lead to an increase in power draw. However, increasing the mill speed from 55 to 75% will lead to an increase in the fractal dimension, reduction

ratio, and weight content of particles smaller than 25 microns. However, increasing the mill speed from 75 to 95% will not affect these parameters and will only lead to an increase in power draw.

References

[1] T. Napier-Munn, S. Morrell, R.D. Morrison, T. Kojovic, Mineral comminution circuits: their operation and optimisation, in, 1996.
[2] D.W. Fuerstenau, J.J. Lutch, A. De, The effect of ball size on the energy efficiency of hybrid high-pressure roll mill/ball mill grinding, Powder Technology, 105(1) (1999) 199–204.
[3] R.P. King, Comminution and liberation of minerals, Minerals Engineering, 7(2) (1994) 129–140.
[4] S. Sadrai, J.A. Meech, M. Ghomshei, F. Sassani, D. Tromans, Influence of impact velocity on fragmentation and the energy efficiency of comminution, International Journal of Impact Engineering, 33(1) (2006) 723–734.
[5] A.S. Erdem, Ş.L. Ergün, The effect of ball size on breakage rate parameter in a pilot scale ball mill, Minerals Engineering, 22(7) (2009) 660–664.
[6] J. Kano, H. Mio, F. Saito, Correlation of grinding rate of gibbsite with impact energy of balls, AIChE Journal, 46(8) (2000) 1694–1697.
[7] S. Cayirli, Influences of operating parameters on dry ball mill performance, Physicochemical Problems of Mineral Processing, 54(3) (2018) 751–762.
[8] G.S. Abdelhaffez, A.A. Ahmed, H.M. Ahmed, Effect of Grinding Media on the Milling Efficiency of a Ball Mill, Rudarsko-Geolosko-Naftni Zbornik, 37 (2022) 171–177.
[9] C.T. Jayasundara, R.Y. Yang, A.B. Yu, J. Rubenstein, Effects of disc rotation speed and media loading on particle flow and grinding performance in a horizontal stirred mill, International Journal of Mineral Processing, 96(1) (2010) 27–35.
[10] D.S. Fortsch, Ball charge loading - Impact of specific power consumption and capacity, 2006.
[11] V. Deniz, The effect of mill speed on kinetic breakage parameters of clinker and limestone, Cement and Concrete Research, 34(8) (2004) 1365–1371.
[12] Y. Kaya, V. Kobya, A. Mardani, N. Mardani, H.E. Beytekin, Effect of Grinding Conditions on Clinker Grinding Efficiency: Ball Size, Mill Rotation Speed, and Feed Rate, Buildings, 14(8) (2024) 2356.
[13] T.I. Martinovic, J.A. Herbst, Y.C. Lo, Optimization of Regrinding Ball Mills at Carol Pellet Plant of the Iron Ore Company of Canada, in, Society for Mining, Metallurgy & Exploration, 1990.
[14] P.-O. Samskog, J. Bjorkman, J. Herbst, Y. Lo, Optimization of the grinding circuit at the Kiruna Plant of LKAB using modeling and simulation techniques, (1990) 279–287.
[15] P.M.C. Faria, R.K. Rajamani, L.M. Tavares, Optimization of Solids Concentration in Iron Ore Ball Milling through Modeling and Simulation, Minerals, 9(6) (2019) 366.
[16] I. Iwasaki, S.C. Riemer, J.N. Orlich, Effects of percent solids and mill loading on ball wear in laboratory taconite grinding, Mining, Metallurgy & Exploration, 2(3) (1985) 185–192.
[17] R. Klimpel, Slurry rheology influence on the performance of mineral/coal grinding circuits, (1983).
[18] C. Tangsathitkulchai, L.G. Austin, Slurry density effects on ball milling in a laboratory ball mill, Powder Technology, 59(4) (1989) 285–293.
[19] F.K. Mulenga, An attainable region perspective on the role of residence time distribution in ball milling, South African Journal of Chemical Engineering, 33 (2020) 125–132.
[20] F. Shi, Slurry rheology and its effects on grinding, (1995).
[21] F.N. Shi, T.J. Napier-Munn, A model for slurry rheology, International Journal of Mineral Processing, 47(1) (1996) 103–123.
[22] A. Makokha, D. Starovoytova, S. Namango, E. Ataro, Effect of Slurry Solids Concentration and Ball Loading on Mill Residence Time Distribution, 2014 (2014) 21–27.
[23] J. Zhao, J. Liu, J. Wang, J. Hou, Energy consumption model of coal grinding based on energy dissipation fractal dimension, Particulate Science and Technology, 42(2) (2024) 301–310.
[24] M. AmanNejad, K. Barani, Effects of Ball Size Distribution and Mill Speed and Their Interactions on Ball Milling Using DEM, Mineral Processing and Extractive Metallurgy Review, 42(6) (2021) 374–379.

[25] S. Tarasiewicz, P. Radziszewski, Comminution energetics part III : Bond's law and breakage energy, Materials Chemistry and Physics, 25(1) (1990) 21–25.
[26] H. Nematollahi, Mineral Processing (In Persian), 6 ed., University of Tehran Press, 2015.
[27] H.E. Rose, D.E. Evans, The Dynamics of the Ball Mill: Part I: Power Requirements Based on the Ball and Shell System, Proceedings of the Institution of Mechanical Engineers, 170(1) (1956) 773–783.
[28] S. Morrell, The Prediction of Power Draw in Wet Tumbling Mills, 1993.
[29] M.H. Moys, A Model Of Mill Power As Affected By Mill Speed, Load Volume, And Liner Design, in, The Southern African Institute of Mining and Metallurgy, 1993.
[30] M.A. van Nierop, G. Glover, A.L. Hinde, M.H. Moys, A discrete element method investigation of the charge motion and power draw of an experimental two-dimensional mill, International Journal of Mineral Processing, 61(2) (2001) 77–92.
[31] T. Allen, Particle Size Measurement, Springer Netherlands, 2012.
[32] I. Moradi, M. Irannajad, Comparison of Size Distribution Description Methods of Jaw and Roll Crushers Products, in: 8th Iranian Mining Engineering Conference, Birjand, Iran, 2020.
[33] I. Moradi, M. Irannajad, Comparison of particle size distribution of jaw and cone crusher's products by same setting and feed size distribution, in: The 3rd Iranian Mining Technologies Conference, Yazd, Iran, 2022.
[34] I. Moradi, M. Irannajad, Effect of Feed Rate on Comminution Products by Fractal Geometry, Amirkabir Journal of Civil Engineering, 53(5) (2021) 2043–2062.
[35] I. Moradi, M. Irannajad, Fractal dimension of crushing products: effects of feed size distribution and feed rate, Particulate Science and Technology, 39(7) (2021) 877–886.
[36] I. Moradi, M. Irannajad, Effect of feed size distribution on the particle size distribution of dry ball mill product by fractal approach, in: 3rd National Conference on Materials Engineering, Metallurgy & Mining, Ahvaz, Iran, 2020.
[37] I. Moradi, M. Irannajad, Description of particle morphology in mineral processing operations by fractal geometry, in: 3rd National Conference on Materials Engineering, Metallurgy & Mining, Ahvaz, Iran, 2020.
[38] I. Moradi, M. Irannajad, Effect of Setting Size and Feeding Rate of Jaw Crusher on Particle Size Distribution by Fractal Geometry, in: 8th Iranian Mining Engineering Conference, Birjand, Iran, 2020.
[39] I. Moradi, M.H. Mohammadzadeh, M. Irannajad, Calculation of fractal dimension of crushing product by variation of ore type and feed size, in: The 2nd Iranian Conference of Green Mining &Mine Industry, Zanjan, Iran, 2019.
[40] E. Hamzelo, M. Masinaei, N. Mehrshad, Discrimination and Identification of Hydrothermal Alteration Types Related to Porphyry Copper Deposits, Using Hyperion Hyperspectral Data, Journal of Mining Engineering, 8(19) (2013) 25–33.
[41] K.J. Falconer, Fractals: A Very Short Introduction, OUP Oxford, 2013.
[42] E. Goudeli, M.L. Eggersdorfer, S.E. Pratsinis, Coagulation–Agglomeration of Fractal-like Particles: Structure and Self-Preserving Size Distribution, Langmuir, 31(4) (2015) 1320–1327.
[43] Z. Jing, F. Xiao-heng, W. Jie, F. Zhi-yuan, Z. Jia-yun, Effect of shear force field on the separation effect of ultra-clean coal based on fractal dimension of flocs, Journal of China Coal Society, (8) (2016) –.
[44] A. Taşdemir, Fractal evaluation of particle size distributions of chromites in different comminution environments, Minerals Engineering, 22(2) (2009) 156–167.
[45] I. Moradi, M. Irannajad, Fractal approach of particle size distribution description of ball milling products: effects of ore type, feed and particle size, Canadian Metallurgical Quarterly, 63(1) (2024) 163–173.
[46] I. Moradi, F. Inanloo S A, M. Irannajad, Effect of dry ball mill on magnetic separator with particle fractal dimension, in: 9th International Conference & Exhibition on Materials Science & Metallurgical Engineering (iMat2020), Tehran, Iran, (2020).
[47] F. Inanloo S. A, I. Moradi, M. Irannajad, Effect of particle shape produced from wet ball milling on magnetic separation concentrate by fractal dimension, Particulate Science and Technology, 42(6) (2024) 978–987.

[48] I. Moradi, M. Irannajad, Effect of wet ball milling on copper ore flotation by fractal geometry, Separation Science and Technology, 58(8) (2023) 1473–1490.
[49] E. Stamboliadis, E. Petrakis, O. Pantelaki, Variation of dimensional properties of particulate materials during grinding and their non-fractal nature, Canadian Metallurgical Quarterly, 50(2) (2011) 119–126.
[50] A.F. Glazner, R.D. Mills, Interpreting two-dimensional cuts through broken geologic objects: Fractal and non-fractal size distributions, Geosphere, 8(4) (2012) 902–914.
[51] I. Moradi, A.A. Abdollahzadeh, M. Irannajad, Computation of fractal dimension and power draw of regrinding depending on particle size distribution, Scientific Reports, 15(1) (2025) 14095.
[52] B.B. Mandelbrot, The Fractal Geometry of Nature, Henry Holt and Company, 1983.
[53] D.L. Turcotte, Fractals and fragmentation, Journal of Geophysical Research, 91 (1986) 1921–1926.
[54] J.P. Hyslip, L.E. Vallejo, Fractal analysis of the roughness and size distribution of granular materials, Engineering Geology, 48(3) (1997) 231–244.
[55] S.W. Tyler, S.W. Wheatcraft, Fractal Scaling of Soil Particle-Size Distributions: Analysis and Limitations, Soil Science Society of America Journal, 56(2) (1992) 362–369.
[56] A. Carpinteri, N. Pugno, A fractal comminution approach to evaluate the drilling energy dissipation, International Journal for Numerical and Analytical Methods in Geomechanics, 26(5) (2002) 499–513.
[57] A. Carpinteri, N. Pugno, A multifractal comminution approach for drilling scaling laws, Powder Technology, 131(1) (2003) 93–98.
[58] A. Carpinteri, G. Lacidogna, N. Pugno, Scaling of energy dissipation in crushing and fragmentation: a fractal and statistical analysis based on particle size distribution, International Journal of Fracture, 129(2) (2004) 131–139.
[59] P. Lu, I.F. Jefferson, M.S. Rosenbaum, I.J. Smalley, Fractal characteristics of loess formation: evidence from laboratory experiments, Engineering Geology, 69(3) (2003) 287–293.
[60] H.A. Ahmed, J. Drzymala, Two-dimensional fractal linearization of distribution curves, Physicochemical Problems of Mineral Processing, 39 (2005) 129–139.
[61] J. Lux, B. Clermont, The influence of mill speed and pulp density on the grinding efficiency for secondary stage grinding, micron, 70(68.6) (2004) 71.76.
[62] B.A. Wills, J.A. Finch, Chapter 7 - Grinding Mills, in: Wills' Mineral Processing Technology (Eighth Edition), Butterworth-Heinemann, Boston, 2016, pp. 147–179.
[63] T. Yoshida, F. Kuratani, T. Ito, K. Taniguchi, Vibration characteristics of an operating ball mill, Journal of Physics: Conference Series, 1264(1) (2019) 012016.
[64] B. Shahbazi, M. Jafari, M. Parian, J. Rosenkranz, S. Chehreh Chelgani, Study on the impacts of media shapes on the performance of tumbling mills – A review, Minerals Engineering, 157 (2020) 106490.